Difference in the relative response of the alanine dosimeter to megavoltage x-ray and electron beams

2013 Phys. Med. Biol. 58 3259

(http://iopscience.iop.org/0031-9155/58/10/3259)

Phys. Med. Biol. **58** (2013) 3259–3282 doi:10.1088/0031-9155/58/10/3259

Difference in the relative response of the alanine dosimeter to megavoltage x-ray and electron beams

M Anton[1], R-P Kapsch[1], A Krauss[1], P von Voigts-Rhetz[2], K Zink[2] and M McEwen[3]

[1] Physikalisch-Technische Bundesanstalt, Bundesallee 100, D-38116 Braunschweig, Germany
[2] Institut für Medizinische Physik und Strahlenschutz (IMPS), University of Applied Sciences Giessen-Friedberg, Wiesenstr 14, D-35390 Giessen, Germany
[3] Ionizing Radiation Standards, National Research Council, Ottawa, Canada

E-mail: mathias.anton@ptb.de

Received 24 October 2012, in final form 14 March 2013
Published 24 April 2013
Online at stacks.iop.org/PMB/58/3259

Abstract

In order to increase the usefulness of the alanine dosimeter as a tool for quality assurance measurements in radiotherapy using MV x-rays, the response with respect to the dose to water needs to be known accurately. This quantity is determined experimentally relative to ^{60}Co for 4, 6, 8, 10, 15 and 25 MV x-rays from two clinical accelerators. For the calibration, k_Q factors for ionization chambers with an uncertainty of 0.31% obtained from calorimetric measurements were used. The results, although not inconsistent with a constant difference in response for all MV x-ray qualities compared to ^{60}Co, suggest a slow decrease from approximately 0.996 at low energies (4–6 MV) to 0.989 at the highest energy, 25 MV. The relative uncertainty achieved for the relative response varies between 0.35% and 0.41%. The results are confirmed by revised experimental data from the NRC as well as by Monte Carlo simulations using a density correction for crystalline alanine. By comparison with simulated and measured data, also for MeV electrons, it is demonstrated that the weak energy dependence can be explained by a transition of the alanine dosimeter (with increasing MV values) from a photon detector to an electron detector. An in-depth description of the calculation of the results and the corresponding uncertainty components is presented in an appendix for the interested reader. With respect to previous publications, the uncertainty budget had to be modified due to new evidence and to changes of the measurement and analysis method used at PTB for alanine/ESR.

1. Introduction

Dosimetry using alanine with read-out via electron spin resonance (ESR) is a convenient tool for quality assurance measurements for radiotherapy. The main reasons are the good

water-equivalence of alanine, the weak dependence on the irradiation quality, non-destructive read-out (different from thermoluminescence detectors) and the small size of the detectors.

Irradiation induces free radicals in the amino acid alanine. The radicals are stable: if the detectors are stored in a dry environment, the fading, i.e. the loss of radicals, is only of the order of a few parts in 10^3 per year, which makes them suitable for mailed dosimetry. The read-out is usually performed by ESR. Since the reading is not absolute, the ESR amplitude has to be calibrated.

Since the 1980s, alanine dosimetry has been used for (mailed) dosimetry for radiation processing, since the mid-nineties, the National Physical Laboratory (NPL, UK) (Sharpe *et al* 1996) and others (De Angelis *et al* 2005, Onori *et al* 2006) also have used alanine for mailed dosimetry in the therapy dose range, i.e. with doses lower than 10 Gy. Recently, advanced therapy modalities such as intensity modulated radiotherapy or the Cyberknife have been checked using alanine dosimetry (Budgell *et al* 2011, Garcia *et al* 2011). A large fraction of the Belgian therapy centres participated in a dosimetry audit using alanine/ESR (Schaeken *et al* 2011).

Several publications deal with the response of the alanine dosimeter to high-energy x-rays and megavoltage electrons, which are the radiation qualities for which the alanine dosimeter is best suited. The energy dependence is very weak. Between ^{60}Co (average photon energy 1.25 MeV) and 25 MV x-rays, the relative response of the alanine dosimeter varies by less than 1% (Sharpe 2003, Bergstrand *et al* 2003, Zeng *et al* 2004, Anton *et al* 2008). None of the listed publications gave evidence of a significant energy dependence for MV x-rays, which is why Sharpe (2003, 2006) from NPL suggested to use a common relative response of 0.994 for all MV qualities[4]. There were no contradictory results reported so far.

For electrons, the situation is similar, the most accurate measurements were published by the National Research Council (NRC, Canada) (Zeng *et al* 2004) and by the Swiss metrology institute METAS in cooperation with PTB (Vörös *et al* 2012). The results presented in these two publications agree (on average) within 0.1% and indicate that a common relative response of 0.988 for all megavoltage electron qualities will be appropriate, with an uncertainty of approximately 1%.

In spite of this apparent consensus situation we used the new electron accelerator facilities at PTB to determine the relative response of the alanine dosimeter for six qualities, namely 4, 6, 8, 10, 15 and 25 MV x-rays. The motivation for the new measurements was that more accurate values for the quality correction factor k_Q for ionization chambers are now available from measurements with the PTB water calorimeter, the uncertainty of the k_Q is 0.31% for all listed qualities. Due to the comparatively large number of measurements made and hence a small statistical uncertainty, a weak energy dependence, i.e. a small drop of the relative response for qualities with an accelerating voltage between 8 and 15 MV, could be identified.

In addition, data for 8 and 16 MV that had been published previously (Anton *et al* 2008) had to be revised. For 8 MV, there was no change apart from a slight increase of the uncertainty. The 16 MV value had to be corrected due to a wrong conversion factor that had been applied to the old data. A comparison between NRC and PTB is also reported; alanine dosimeter probes were irradiated at NRC and analysed at PTB. This was prompted by apparent discrepancies between the 25 MV results published by NRC (Zeng *et al* 2004) and our new data.

Monte Carlo simulations were carried out in order to find out whether the observed behaviour of the alanine dosimeter could be reproduced by the calculations. Zeng *et al* (2005) showed that it was necessary to use the density effect correction for crystalline alanine instead of

[4] This means that the dose determined by an alanine dosimeter—with a calibration using ^{60}Co—has to be multiplied by 1.006 in order to yield the correct dose. The uncertainty of Sharpe's data is 0.6%.

Table 1. Properties of the Harwell alanine pellets used.

Batch	Average mass (mg)	Diameter (mm)	Height (mm)	Density ($g\,cm^{-3}$)	CV (%)
AF594	59.4 ± 0.2	4.82 ± 0.01	2.8 ± 0.1	1.16	0.4
AJ598	59.8 ± 0.2	4.82 ± 0.01	2.7 ± 0.1	1.21	0.4
AL595	59.5 ± 0.2	4.82 ± 0.01	2.6 ± 0.1	1.25	0.3

a density effect correction for the alanine/paraffin mixture with the bulk density of the pellet in order to reproduce the relative response for high energy electrons. Therefore, calculations with the different density corrections were compared for the MV x-ray qualities under investigation. Additional simulations were made to determine some parameters of interest such as stopping power ratios, the mean secondary electron energy and electron ranges, which helped to explain the new results.

In an appendix, the uncertainty budget is detailed. This appeared necessary due to new evidence as well as to a slightly modified measurement and analysis method. Using the dose-normalized amplitude directly instead of a complete calibration curve saves several hours of measurement time per day and leads only to a moderate, but acceptable increase of the overall uncertainty. Details of the experimental results are also only given in the appendix. This will facilitate the reading of the main text, but will provide the interested reader with all the information necessary to follow the calculation of the results and their uncertainties. All uncertainties are standard uncertainties (coverage factor $k = 1$) and are determined according to the terms of reference stated in the *GUM*, the *Guide to the expression of uncertainty in measurement* (JCGM100 2008).

For the sake of simplicity, *dose* or D is to be understood as *absorbed dose to water* in the following, unless otherwise stated.

2. Materials and methods

2.1. Dosimeter probes

Alanine pellets with an addition of approximately 9% of paraffin as a binder, supplied by Harwell, were used. Their parameters are listed in table 1. The leftmost column lists the name of the batch. The following columns are the average mass in mg and the dimensions in mm. The rightmost column, denoted as CV (= coefficient of variation), quantifies the uncertainty of the intrinsic response, i.e. the signal per mass if the same dose is applied to different pellets of the same batch. This is due to variations of the composition. The CV value is usually specified by the supplier. An experimental verification for batch AL595 yielded the same CV of 0.3%. The uncertainty for an individual mass is estimated as $60\,\mu g$ and takes the loss of material due to handling for up to ten handling processes into account (see Anton 2005). Test pellets (irradiated in MV x-ray fields) and calibration pellets (irradiated in the ^{60}Co reference field) were always taken from the same batch.

One detector consists of a stack of four alanine pellets that has to be protected from the surrounding water. All detectors that were used for the determination of the relative response were irradiated in a polymethylmethacrylate (PMMA) holder fitting inside a watertight PMMA sleeve for a NE 2571 (Farmer) ionization chamber (see Anton 2006). A small additional set of detectors shrink-wrapped in polyethylene (PE) was irradiated. The detectors together with their holder are referred to as *probes*.

The two different probes are shown as schematic drawings (to scale) in figure 1. Panel (a) shows the detector with a Farmer holder and sleeve with a total PMMA wall thickness of 2 mm.

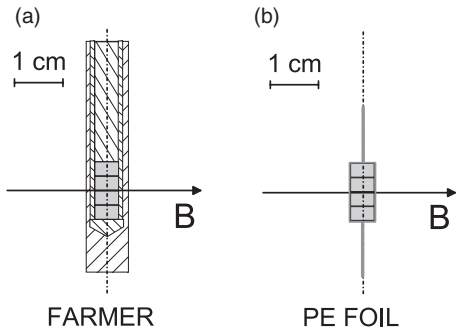

Figure 1. Different probes used—panel (a) detector with a PMMA holder fitting in a watertight sleeve for a Farmer chamber; panel (b) a detector shrink-wrapped in 0.2 mm strong PE foil. The capital B denotes the beam axis, the dash-dotted line indicates the symmetry axis of the detector.

Panel (b) shows a sketch of the PE foil probe. The thickness of the PE foil is 0.18–0.20 mm (photograph see Vörös *et al* 2012). A possible influence of the holder on the relative response of the alanine dosimeter was investigated for ^{60}Co, 4 and 25 MV radiation.

2.2. Irradiation in the reference fields of the PTB

2.2.1. Irradiations in the ^{60}Co *reference field.* The calibration probes were irradiated in the ^{60}Co reference field. The field size was 10 cm × 10 cm at the reference depth of 5 cm. The geometrical centre of the probes (see figure 1) was placed at the reference depth in a 30 cm × 30 cm × 30 cm cubic water phantom.

The contribution to the relative uncertainty of the delivered dose of 0.05% is due to positioning uncertainties. The lateral dose profile (in the plane perpendicular to the beam axis) over the volume of the alanine probe and over the sensitive volume of a Farmer chamber is flat, no correction and no additional uncertainty contribution had to be taken into account.

The relative uncertainty of the absorbed dose to water as determined with the PTB water calorimeter is 0.2% (Krauss 2006). Taking an additional small contribution for the source shutter into account led to a relative uncertainty of the delivered dose of 0.22%.

2.2.2. Irradiations in MV x-ray fields. Photon beams with nominal accelerating voltages of 4, 6, 8, 10, 15 and 25 MV were supplied by two *Elekta Precise* linear accelerators. Irradiations were performed at the reference depth of 10 cm in a cubic water phantom (30 cm edge length) with a source-surface distance of 100 cm. The field size was 10 cm × 10 cm at the reference depth. The dose rate at the reference depth was set to a value between 1 and 2 Gy min^{-1}. The tissue-phantom ratio TPR_{10}^{20} for each quality was determined experimentally.

All measurements performed at the linear accelerators are normalized to the reading of a large-area transmission ionization chamber which was calibrated every day via a secondary standard ionization chamber before *and* after the irradiations of the alanine pellets. In most cases, a Farmer NE 2571 chamber was used but for a few irradiations a watertight IBA FC65-G chamber was employed. For the reproducibility of the dose, an uncertainty component of 0.12% was estimated (see Krauss and Kapsch 2007).

For the individual ionization chambers used, quality correction factors k_Q had been determined using the water calorimeter. The uncertainty of the k_Q values for the 10 cm × 10 cm

Table 2. Non-uniformity correction: ratio of dose averaged over the volume of the four alanine pellets to the dose averaged over the volume of a Farmer chamber.

MV	D_{det}/D_{ic}	u	u_{indep}
4	1.0009	0.0001	0.0009
6	1.0002	0.0003	0.0008
8	1.0008	0.0001	0.0009
10	0.9980	0.0002	0.0013
15	1.0000	0.0001	0.0008
25	0.9984	0.0002	0.0010

field is 0.31%[5]. The uncertainty of the ^{60}Co calibration coefficient for the reference ion chambers NE 2571 and FC65-G is 0.25%.

For all MV beams used, the dose distribution in the reference depth in a plane vertical to the beam axis was measured. From these distributions, non-uniformity corrections were calculated by numerical integration over the sensitive volume of the ionization chamber and the alanine detector. The ratio D_{det}/D_{ic} of the dose integrated over the alanine detector D_{det} and over the ionization chamber D_{ic} is listed in table 2. The absorbed dose as determined by the ionization chamber has to be multiplied by that ratio in order to obtain the absorbed dose for the alanine detector.

The uncertainty of this correction, due to positioning uncertainties of the probes, was determined using Monte Carlo methods. A positioning uncertainty of 1 mm in both directions perpendicular to the beam axis was assumed. The column u lists the resulting uncertainty of D_{det}/D_{ic} for the usual case when both chamber and alanine were irradiated in the same sleeve. The column u_{indep} is required for the single case (15 MV, hl15 of 2012-01-26 in table A4) when ionization chamber and alanine were positioned independently, hence the index $_{indep}$.

The uncertainty contribution from the depth determination was comparable to the one for the ^{60}Co field due to similar gradients of the depth dose curves.

2.2.3. Irradiation temperature. The irradiation temperature is an important influence quantity for alanine dosimetry and was registered with an uncertainty of 0.1 °C. Since it was only possible to measure the temperature of the surrounding water, a time delay of 10 min is usually inserted between the placing of the detector in the water and the beginning of the irradiation. For the measurements in the cobalt reference field and at the accelerators two different sensors were used.

2.3. ESR measurements and analysis

ESR measurements were performed usually one or two weeks after irradiation, using a Bruker EMX 1327 ESR spectrometer, with an 8″ magnet and an X-band microwave bridge. The high-sensitivity resonator ER 4119 HS was used throughout. The measurement parameters are listed in a previous publication (Anton 2006), which also contains a detailed description of the hardware and the evaluation method.

To a measured spectrum—which contains the signal contributions from both the irradiated alanine (ala) and from a reference substance (ref)—two base functions are fitted, thereby yielding the corresponding coefficients A^{ala} and A^{ref}. The base functions, one containing

[5] These results remain to be published in a separate paper. A similar uncertainty budget is detailed in the publication cited above (Krauss and Kapsch 2007), but for the k_Q-factors determined at the PTB's former linear accelerator.

a pure alanin signal, one containing the signal of the reference (plus background), are determined experimentally from spectra of unirradiated pellets and from spectra of alanine pellets irradiated in the ^{60}Co reference field to 25 Gy. Four to eight pellets with a dose of 25 Gy as well as the same number of unirradiated ones have to be measured on the same day as the test pellets. Examples for the base functions were displayed in previous publications (Anton 2005, 2006).

The readings from the four pellets making up one detector are averaged to yield the dose-normalized amplitude $\mathcal{A}_D$, which is defined as

$$\mathcal{A}_D = \frac{A_m}{\overline{m}} \cdot k_T \cdot \frac{\overline{m}^{\mathrm{b}}}{k_T^{\mathrm{b}}} \cdot D^{\mathrm{b}}. \tag{1}$$

The index b refers to the base function. $A_m = \overline{m} \sum A_i/m_i$ is the mass-normalized amplitude for one detector ($A_i = A^{\mathrm{ala}}/A^{\mathrm{ref}}$, $i = 1 \ldots n = 4$ pellets), $\overline{m}$ and $\overline{m}^{\mathrm{b}}$ are the average masses of test and base function detectors, respectively, and k_T and k_T^{b} are the corresponding temperature correction factors (temperature correction coefficient taken from Krystek and Anton (2011)).

Usually, the dose-normalized amplitude (1) serves to set up a calibration curve with a resulting measurement function (Anton 2006)

$$D^{\mathrm{c}} = N \cdot \mathcal{A}_D + D_0. \tag{2}$$

The upper index c is used to distinguish the calculated dose D^{c} from the delivered dose D. Ideally, we would have $N = 1, D_0 = 0$ due to the definition of $\mathcal{A}_D$. This ideal measurement curve is implicitly assumed if $\mathcal{A}_D$ is identified with D^{c}. Compared to measurements using a complete calibration curve, direct use of $D^{\mathrm{c}} = \mathcal{A}_D$ reduces the time required for calibration by at least 2 h per day. The price to pay for the reduced measurement time is a slightly higher uncertainty. The measurement results presented below contain data evaluated with an explicit calibration curve as well as data where $D^{\mathrm{c}} = \mathcal{A}_D$ was used directly (which method was used for which dataset is explained in section A.3).

2.4. The relative response

From the determined dose D^{c} and the known value of the delivered dose D, an empirical value r of the relative response is simply

$$r = \frac{D^{\mathrm{c}}}{D}. \tag{3}$$

Due to the calibration as described (^{60}Co base, ^{60}Co calibration curve, ionization chamber calibrated to indicate dose to water for the quality under consideration), r represents the relative response with respect to the dose to water, relative to ^{60}Co-radiation. The response thus determined is dependent not only on the material but also on the geometry of the detector. The correction factors for alanine detector arrangements with a completely different geometry (different size, more massive holder) may differ from the values presented in this study.

In order to determine a reliable value $\langle r \rangle_Q$ for the relative response for every quality Q, several separate values $r_{j,Q}$ were obtained (the subscript $_Q$ is dropped for the sake of simplicity in the following). Between $n_j = 4$ and $n_j = 9$ values were produced for every quality. Every value r_j is obtained from one irradiation set, i.e. a set of test probes, comprising $n_i = 3 \ldots 8$ detectors irradiated to dose values between 5 and 20 Gy on the same day, plus some irradiated detectors required for the calibration as outlined above. The determination of $\langle r \rangle$ as well as the uncertainty budget are detailed in the appendix.

Table 3. Relative response of alanine to MV x-rays. Columns from left to right: nominal accelerating voltage in MV; tissue-phantom ratio TPR_{10}^{20}; dose-to-water response relative to ^{60}Co-radiation $\langle r \rangle$; the uncertainty component u or u_{mod} from (A.1) or (A.6) (see appendix), the combined uncertainty $u(\langle r \rangle)$ including the uncertainties of the calibration factor and k_Q for the ionization chambers; square sum of residuals q^2 from (A.5); number of datasets n_j; finally whether the q^2 criterion was satisfied.

	MV	TPR_{10}^{20}	$\langle r \rangle$	u or u_{mod}	$u(\langle r \rangle)$	q^2	n_j	$q^2 < n_j - 1$?
	4	0.638	0.9953	0.0010	0.0036	2	4	y
	6	0.683	0.9970	0.0007	0.0035	6.5	9	y
	8	0.714	0.9958	0.0022	0.0041	9.8	5	n
(2008 rev.)	8	0.716	0.9959	0.0022	0.0041	4.8	4	n
	10	0.733	0.9940	0.0011	0.0036	10.0	8	n
	15	0.760	0.9890	0.0011	0.0036	2.9	6	y
(2008 rev.)	16	0.762	0.9908	0.0010	0.0035	0.1	4	y
	25	0.799	0.9893	0.0012	0.0036	7.9	7	n

3. Results and discussion

3.1. Experimental results

The results of each individual irradiation and measurement set j are listed in tables A3 and A4 of section A.3. The final result $\langle r \rangle$, the relative response averaged over all n_j data sets obtained for a specific quality, is shown in table 3. The leftmost column lists the nominal accelerating voltage in MV, the following column represents the tissue-phantom ratio TPR_{10}^{20}. The third column contains $\langle r \rangle$, the following column lists u or u_{mod} according to equations (A.4) and (A.6), respectively. The combined uncertainty $u(\langle r \rangle)$ contains also the uncertainty of the calibration of the ionization chamber and the uncertainty of the quality correction factors k_Q for each quality. The values of the parameter q^2 (A.5) and the number of datasets n_j are displayed in the following columns, the rightmost column indicates whether the consistency criterion according to (A.5) was satisfied (y) or not (n). If not, u_{mod} according to equation (A.6) was used instead of u from (A.4) as the uncertainty of the weighted mean, which was the case for 8, 10 and 25 MV[6]. Only for 8 MV u_{mod} was significantly larger than u. However, the effect is not dramatic for the overall uncertainty $u(\langle r \rangle)$.

In addition to the new measurements, the results that had been published earlier (Anton *et al* 2008) had to be revised. They are also contained in table 3 and labelled (2008 rev.). There is no change in the old 8 MV data, the published value was 0.9959 which is identical to the revised result. The uncertainty turned out to be higher than previously published, the new value is 0.0041 whereas the published value was 0.0028. One of the main reasons for this increase is that the uncertainty contributions from the intrabatch homogeneity and the calibration factor of the ionization chamber had been erroneously omitted. The situation is more dramatic for the 16 MV data, the response changed from the published value 0.9967 ± 0.0027 to the revised value of 0.9908 ± 0.0035. The value of the published 16 MV response was in error, due to an incorrect conversion factor that had been used. The reasons for the modified uncertainty are the same as for the 8 MV value.

The data from table 3 are displayed in figure 2 as a function of the tissue-phantom ratio. The reference, ^{60}Co-radiation, is represented by the filled circle. Filled triangles indicate the

[6] This was already the case for the 8 MV data published earlier (Anton *et al* 2008). There is still no evidence as to which of the uncertainty components might be underestimated. A significant amount of work was invested in testing different options. Reporting all these attempts to identify the unknown source(s) would be outside the scope of this publication.

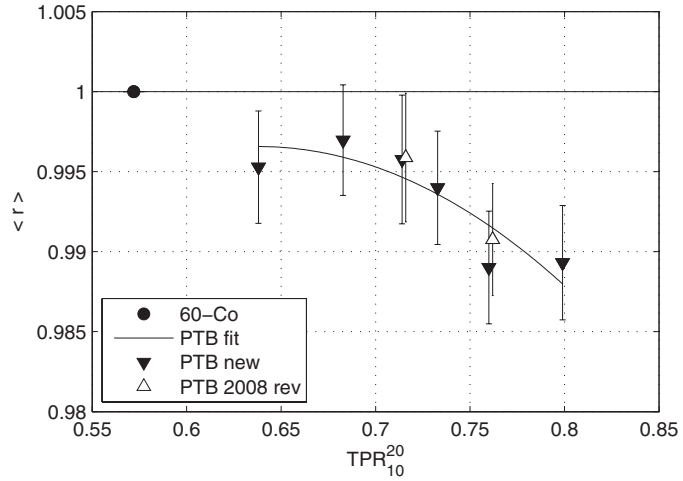

Figure 2. The relative response $\langle r \rangle$ and its uncertainty as a function of TPR^{20}_{10}. The reference ^{60}Co is indicated by the filled circle, the new data are represented by the filled triangles. The revised values of our 2008 data are added as open triangles. The fit curve is only shown to guide the eye and for later comparisons.

Table 4. Mean ratio $\mathcal{R}_{\mathrm{PE,Farmer}}$ as defined in (4) and its uncertainty for three different radiation qualities Q.

Q	$\mathcal{R}_{\mathrm{PE,Farmer}}$	$u(\mathcal{R}_{\mathrm{PE,Farmer}})$
^{60}Co	0.9997	0.0016
4 MV	0.9993	0.0019
25 MV	1.0014	0.0018

new values, open triangles represent the revised 2008 data. The error bars correspond to $u(\langle r \rangle)$ according to table 3. A parabolic curve which was obtained by a least-squares fit to the data is also shown, only to guide the eye. For the lower energies, the response values are consistent with the recommendation of Sharpe while the value for the highest energy is interestingly similar to the value obtained for the response to high-energy (MeV) electrons (Vörös *et al* 2012).

3.2. Comparison of different holders

For three qualities, namely ^{60}Co, 4 and 25 MV, several detectors were irradiated with doses between 10 Gy and 25 Gy, but in two different holders. One was the Farmer holder with a wall thickness of 2 mm, the other one was a shrink-wrapping with 0.2 mm PE (see figure 1). A weighted mean $\langle \mathcal{A}_D/D \rangle$ was calculated for three to four detectors per holder and quality. The uncertainties have been estimated as described in the appendix. The results are summarized in table 4: for each quality the mean ratio

$$\mathcal{R}_{\mathrm{PE,Farmer}} = \frac{\langle \mathcal{A}_D/D \rangle_{\mathrm{PE}}}{\langle \mathcal{A}_D/D \rangle_{\mathrm{Farmer}}} \tag{4}$$

and its uncertainty are given for the three qualities under consideration.

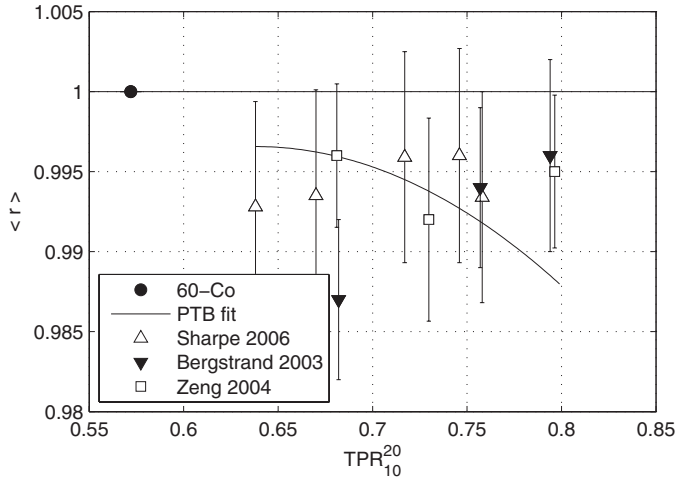

Figure 3. The relative response and its uncertainty as a function of TPR^{20}_{10}. The reference ^{60}Co is indicated by the filled circle. For the sake of clarity, the new PTB data are represented by the fit curve only. Open triangles: NPL, Sharpe (2006) with only approximate TPR values; filled triangles: Bergstrand *et al* (2003); open squares: Zeng *et al* (2004).

Within the limits of uncertainty, no influence of the holder can be discerned. Since the PE foil probe is a very good approximation to using the alanine detector without any holder at all, we concluded that it would be justified to neglect the holder in the Monte Carlo simulations (see section 4). This conclusion may not be valid if a more massive holder (i.e. wall thickness >2 mm) were to be used, although McEwen *et al* (2006) showed that no holder effect was seen in MeV electron fields for sleeve thicknesses up to 4 mm .

3.3. Comparison to other experimental data

For the sake of clarity, the fit curve shown in figure 2 is also used to compare the new results to the results of other authors. In figure 3, published data by Bergstrand *et al* (2003), Zeng *et al* (2004) and by Sharpe (2006) are displayed.

The data from Bergstrand *et al*, which are indicated by the filled triangles, show a trend which is just the inverse of what our new measurements seem to indicate, albeit with the largest uncertainties. The NRC data from Zeng *et al* which are indicated by the open squares and the NPL data which are represented by the open triangles are consistent with the proposal by Sharpe (2006) to use a constant, energy independent response of 0.994 for the whole range of MV therapy qualities.

3.4. NRC—new data and revised results

The systematic nature of the deviation between the new PTB data and those presented in the literature—increasing to ≈0.6% at 25 MV—is grounds for further investigation. Therefore, alanine pellets were irradiated by NRC in the spring of 2012 and evaluated by PTB. The data set comprised four sets of test detectors, one for ^{60}Co-irradiation and one for each of the three nominal voltages of 6, 10 and 25 MV that are available at the NRC's *Elekta Precise* accelerator. Irradiations at NRC were carried out in a similar way as at PTB using a watertight PMMA sleeve for the detector, i.e. a stack of four pellets. For each quality, $n_i = 3$ to $n_i = 4$ detectors

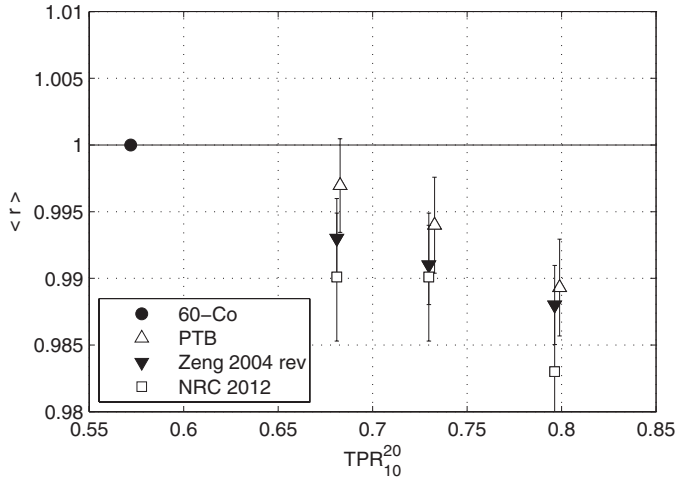

Figure 4. The relative response and its uncertainty as a function of TPR_{10}^{20}. The reference ^{60}Co is indicated by the filled circle. The PTB data are represented by the open triangles. The data obtained using probes irradiated at NRC and evaluated at PTB are represented by the open squares. The revised data from Zeng *et al* (2004) are shown as filled triangles. Error bars indicate the standard uncertainties including the primary standard(s).

Table 5. Relative response values for alanine detectors irradiated at NRC in May 2012 and analysed at PTB.

Quality	TPR_{10}^{20}	n_i	n_c	r_j	$u(r_j)$
^{60}Co	0.572	4	5	0.9999	0.0047
6 MV	0.681	4	5	0.9901	0.0048
10 MV	0.730	3	5	0.9901	0.0048
25 MV	0.796	3	5	0.9830	0.0048

were irradiated with doses of approximately 10, 15 and 20 Gy. Doses were derived from a reference ionization chamber calibrated against the NRC primary standard water calorimeter.

Evaluation and analysis were carried out as outlined above. The results are summarized in table 5. The leftmost column lists the quality. In the next column, the tissue-phantom ratio is given, and n_i and n_c are the number of test- and calibration detectors. The uncertainties were determined as explained in the appendix. They are slightly higher than for the data where irradiation and analysis were both carried out at PTB because two different primary standards are now involved.

From the key comparison BIPM.RI(I)-K4 (absorbed dose to water, primary standards) it was expected that the ^{60}Co-irradiated probes would exhibit a slightly lower signal if evaluated with calibration probes irradiated at PTB (to be precise, a difference of 0.19% was expected). Indeed, the dose ratio ($r_j = 0.9999$) was consistent with this value within the combined standard uncertainty of 0.47%.

The MV data tabulated in table 5 are displayed in figure 4 as open squares. All response values lie below the PTB data for the corresponding qualities which are displayed as open triangles. There is no significant contradiction in view of the uncertainties. If the data in table 5 are compared to the corresponding data in tables A3 and A4, only for 6 MV, the measured value is outside the range of observations at PTB, but still within the limits of uncertainty. Surprisingly the NRC value of r_j is now less than the PTB value at all energies.

Table 6. Relative response for alanine, values as published by Zeng *et al* (2004) and revised values using new k_Q corrections and uncertainties.

		Published		Revised	
Quality	TPR_{10}^{20}	$\langle r \rangle$	u_r in %	$\langle r \rangle$	u_r in %
^{60}Co	0.572	1		1	
6 MV	0.681	0.996	0.45	0.993	0.30
10 MV	0.730	0.992	0.65	0.991	0.30
25 MV	0.796	0.995	0.48	0.988	0.30

Due to this unexpected result, the data published by Zeng *et al* (2004) was revisited and it was found that different k_Q data had been used for the reference ion chamber than had been used for the 2012 irradiations. The high-precision k_Q data presented in McEwen (2010) was not available at the time of the Zeng *et al* irradiations. The revised data are listed along with the published ones in table 6 and displayed as filled triangles in figure 4 (compare figure 3). The revised values are shifted to slightly lower values. The most pronounced change is observed for the 25 MV response which now agrees very well with the new PTB data. In summary, NRC and PTB data appear to agree better than expected from the published data alone. The somewhat higher deviation of the new set of measurements can not be considered a severe problem since the data are equivalent to just one r_j measurement (according to the nomenclature defined in the appendix) whereas the revised published data as well as the measurements presented in this paper represent weighted averages $\langle r \rangle$ over at least 4 r_j-values.

To complete this discussion, one should also consider the potential differences between the NRC and PTB standards in high-energy linac beams, which could speak to the apparent difference between the two laboratories indicated in figure 4. In the both the PTB and NRC irradiations, a calibrated NE2571 ion chamber was used to determine the dose delivered to the alanine pellets and therefore there are a number of sources we can refer to in determining the NRC/PTB dose ratio. Aalbers *et al* (2008) collated k_Q data from a larger number of investigations (but not PTB) and showed that the NRC data were consistent with an unweighted fit of all data at the 0.2% level for 6, 10, and 25 MV beams. Muir *et al* (2011) analysed unpublished data from a large inter-laboratory comparison (including PTB) and showed again that the NRC results were consistent with the global fit (figure 1 of that paper). Although the other lab's results were anonymous it can be seen that there are no significant outliers and therefore one can conclude that the PTB and NRC results are consistent at the 0.3% level. A final comparison is possible through the recently-initiated BIPM.RI(I)-K6 program, where each laboratory's dose standard is compared directly with the BIPM graphite calorimeter. Results for both NRC and PTB are available (Picard *et al* 2010, 2011) and these indicate agreement between the two laboratories within the stated uncertainties. Combining these results one can conclude that the data represented in figure 4 are not sensitive at the 0.3% level to the specific primary standards operated at the two laboratories.

4. Monte Carlo simulations

The apparent decrease in the relative response of alanine for $TPR_{10}^{20} > 0.72$ was unexpected and the literature, based on either Monte Carlo or experimental results (Zeng *et al* 2004, Anton 2006), provided no satisfactory explanation. However, the fact that the asymptotic value of the response for higher energies approaches the one observed for electrons gave a hint towards a

possible explanation: Zeng *et al* (2005) stated in their publication on the relative response of alanine to MeV electron radiation that it was necessary to take the density correction for the crystalline alanine into account. This is justified by the fact that the interactions which produce the free radicals necessarily take place within the alanine microcrystals. In the publication by Vörös *et al* (2012), the density correction for crystalline alanine was also successfully applied but was not explicitly mentioned.

The simulations presented in this work were carried out at the Institut für Medizinische Physik und Strahlenschutz-IMPS (University of Applied Sciences Giessen-Friedberg, Germany) using the EGSnrc package with the user code DOSRZnrc (Kawrakow 2000, Kawrakow *et al* 2010). With DOSRZnrc, the geometry is simplified assuming cylindrical symmetry about the beam axis. The dose scoring volume with a radius and a depth of 5 mm, representing the alanine detector, was placed inside a cylindrical water phantom with a radius of 20 cm and a depth of 30 cm. The geometrical centre of the scoring volume was placed 5 cm behind the phantom surface for the ^{60}Co simulations and 10 cm behind the surface for the MV x-rays. Parallel beams were assumed for the simulation.

For the ^{60}Co reference field, the spectrum was obtained from a MC simulation, taking the realistic geometry of the irradiation source and its surroundings into account. A BEAMnrc (Rogers *et al* 2004) simulation carried out at PTB of one of the *Elekta* accelerators provided the spectra for 6 and 10 MV. For 8 and 16 MV, published spectra had been modified to reproduce the experimental depth dose curves (see Anton *et al* 2008). For the 25 MV beam, a spectrum published by Sheikh-Bagheri and Rogers (2002) was used. For 4 MV, no spectrum was available.

4.1. Simulation of the relative response

For each of the qualities ^{60}Co, 6, 8, 10, 16 and 25 MV, the calculation was carried out three times: the first one for a dose scoring volume made of water to obtain D_{W}; the second and third one with a dose scoring volume consisting of a homogeneous mixture of the atomic constituents of the alanine/paraffin pellets, in order to obtain D_{ala}. Two separate sets for D_{ala} were obtained, one taking the density correction for crystalline alanine into account, the other one using a density correction for the bulk density of the pellets. The calculations were performed with threshold/cut-off energies for the particle transport set to ECUT = AE = 521 keV and PCUT = AP = 1 keV and continued until a preselected statistical uncertainty was achieved. For the other parameters of the simulation, the default settings of DOSRZnrc were used. For each quality, the ratio(s) $D_{\mathrm{ala}}/D_{\mathrm{W}}$ were then calculated and referred to the corresponding ratio for ^{60}Co, i.e. r_Q^{MC}, the simulated dose-to water response for the quality Q, relative to ^{60}Co, is given as

$$r_Q^{\mathrm{MC}} = \frac{(D_{\mathrm{ala}}/D_{\mathrm{W}})_Q}{(D_{\mathrm{ala}}/D_{\mathrm{W}})_{Co}}. \tag{5}$$

The results are displayed in figure 5 along with the previously-shown fit curve to the new PTB data. The results of the DOSRZnrc simulation with the density correction for the bulk density are represented by the open circles whereas the results obtained using the density correction for the crystalline alanine are displayed as filled squares. The error bars indicate the statistical uncertainties. TPR_{10}^{20} values were obtained from simulated depth-dose curves. The data obtained using the bulk density correction are approximately unity and inconsistent with any published experimental results. Within the limits of uncertainty, simulated data using the crystalline alanine density corrections and measured data agree very well. Although this had been pointed out by Zeng *et al* (2005) for MeV electrons already, this finding is new for MV x-rays.

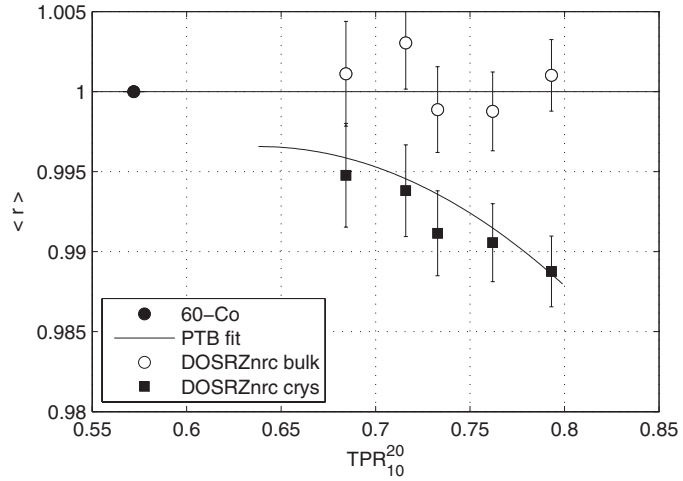

Figure 5. The relative response and its uncertainty as a function of TPR^{20}_{10}. The reference ^{60}Co is indicated by the filled circle. The measured data are represented by the continuous fit curve. MC results obtained using the bulk density correction are shown as open circles, the results obtained using the density correction for crystalline alanine are indicated by the filled squares. The error bars represent the statistical uncertainties.

4.2. Further considerations concerning the possible energy dependence

With the aim to understand the apparent decrease of the relative response of the alanine dosimeter with increasing photon energy, further investigations were made using the MC method.

From the photon spectra that were used for the MC simulations, the spectra in 5 cm depth (Co) and in 10 cm depth (MV x-rays) were calculated using the absorption coefficients compiled and published by the National Institute of Standards and Technology (NIST, USA) based on the publications by Seltzer (1993) and Hubbell (1982). From the attenuated spectra, the average mass energy absorption ratios for alanine and water were determined. The $(\mu_{en}/\rho)_{ala,W}$-ratio is listed in table 8 and displayed in figure 6 as a function of TPR^{20}_{10} (filled circles). With the help of the user codes SPRRZnrc and FLURZnrc from the EGSnrc package, the stopping power ratios $s_{ala,W}$ and the mean electron energies E_{av} in water were also calculated. In table 8 and figure 6, two sets of data for $s_{ala,W}$ are supplied, one using the density correction for the crystalline alanine (designated by *crystal*) the second one using the bulk density of the pellets (designated by *bulk*). The latter are indicated by the open triangles in figure 6, the former are displayed as filled triangles. From the mean secondary electron energy E_{av} listed in table 8, the corresponding electron ranges in the continuous slowing down approximation (CSDA) for the medium water and for alanine (using the same value for the mean energy) were obtained using the NIST/ESTAR database (Berger *et al* 2005) available at the web site of NIST[7]. The CSDA ranges are also given in table 8, converted from g cm^{-2} to cm using the density of water and of alanine (1 and 1.4 g cm^{-3}, respectively).

Finally, we repeated the DOSRZnrc calculation with alanine (crystalline density correction) and with water as a detector material, but with the parameter ECUT set to a value larger than the maximal photon energy *outside* the detector volume. This means all electrons

[7] The stopping powers obtained from the NIST/ESTAR database as well as the density corrections in the EGSnrc software are calculated according to ICRU Report 37 (ICRU 1984).

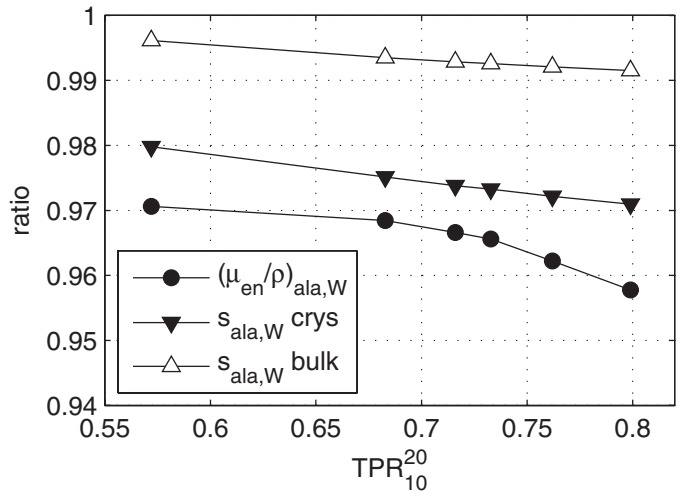

Figure 6. Ratios of mass-energy-absorption coefficients and stopping power ratios for alanine and water. Filled circles: $(\mu_{en}/\rho)_{ala,W}$; filled triangles: $s_{ala,W}$, density correction for crystalline alanine; open triangles: $s_{ala,W}$, density correction for bulk density of the pellet. Lines are shown to guide the eye.

generated outside are not transported and therefore cannot enter the detector volume. We then calculated the ratio of the absorbed dose inside the scoring volume with ECUT = 521 keV inside and with ECUT larger than the maximal photon energy on the outside to the absorbed dose with ECUT = 521 keV everywhere (see the results from the previous section). This yielded the *fraction of the absorbed dose* which is due to the secondary electrons generated by *photon interactions inside* the detector. This fraction is denoted as f_γ in table 8. The values listed are average values for alanine and water as a detector material. For ^{60}Co-radiation, 76% of the dose to the detector are due to secondary electrons that were generated by photon absorption inside the detector volume whereas for the highest energies about 80% of the dose are due to secondary electrons generated outside the detector volume. Speaking in terms of Bragg–Gray theory, the alanine probe becomes an electron probe for the highest voltages. Thus, for the higher energies the relative response should be determined almost exclusively by the stopping power ratio $s_{ala,W}$ and it should approach the value for electrons, which is the case for the experimental data as well as for the simulated ones.

In addition to the photon qualities investigated, the corresponding relevant parameters were also determined for two electron beams with maximum energies of 6 MeV and 18 MeV, using spectra published by Ding *et al* (1995). The parameters obtained for the two electron beams confirm the transition to an electron detector for the higher photon energies as mentioned above, as can be seen by comparing the data in table 8 and in figure 7.

However, it is important to keep in mind that the response thus determined is dependent not only on the material but also on the geometry of the detector. The correction factors for alanine detector arrangements with a completely different geometry (e.g. for much larger detectors or for alanine film dosimeters) may differ from the values presented in this study.

From figure 6 two important facts can be immediately deduced: first, both the $(\mu_{en}/\rho)_{ala,W}$-ratio as well as the stopping power ratio $s_{ala,W}$ *for the crystalline alanine density correction* decrease by approximately 1% between ^{60}Co and 25 MV. Therefore, the observed decrease of the relative response should not be so surprising after all. Second, if we take the ratio as

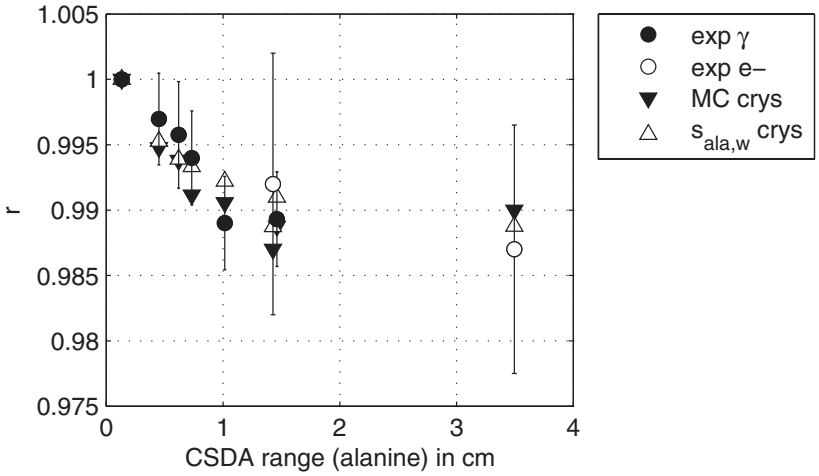

Figure 7. Relative response as a function of the CSDA range in alanine with a density of 1.4 g cm^{-3}, in cm. Filled circles with error bars: experimental data, this work; open circles with error bars: Vörös *et al* (2012) for electrons; filled triangles: MC simulation with density correction for crystalline alanine; open triangles: stopping power ratios $s_{\mathrm{ala},W}$ relative to cobalt, density correction for crystalline alanine.

Table 7. Monte Carlo simulation using DOSRZnrc: for each quality Q the tissue-phantom ratio TPR_{10}^{20} is given along with the simulation results, the ratio $D_{\mathrm{ala}}/D_{\mathrm{W}}$ of the dose to alanine to the dose to water, its relative (statistical) uncertainty and the resulting value of r_Q^{MC}. The left block of data was obtained using the density of crystalline alanine for the density correction, the right block was obtained using the bulk density of the pellets.

		Density of crystalline alanine				Density of pellet bulk			
Q	TPR_{10}^{20}	$D_{\mathrm{ala}}/D_{\mathrm{W}}$	u_r in %	r_Q^{MC}	$u(r_Q^{\mathrm{MC}})$	$D_{\mathrm{ala}}/D_{\mathrm{W}}$	u_r in %	r_Q^{MC}	$u(r_Q^{\mathrm{MC}})$
^{60}Co	0.567	0.9735	0.14			0.9749	0.14		
6 MV	0.660	0.9684	0.30	0.9948	0.0032	0.9760	0.30	1.0011	0.0033
8 MV	0.716	0.9675	0.25	0.9938	0.0029	0.9779	0.26	1.0030	0.0029
10 MV	0.733	0.9649	0.23	0.9911	0.0027	0.9739	0.23	0.9989	0.0027
16 MV	0.762	0.9643	0.21	0.9906	0.0024	0.9737	0.21	0.9988	0.0025
25 MV	0.793	0.9625	0.18	0.9888	0.0022	0.9759	0.18	1.0010	0.0022

approximations to D_{ala}/D_w, both $(\mu_{\mathrm{en}}/\rho)_{\mathrm{ala},W}$ and $s_{\mathrm{ala},W}$ values for cobalt are very close to the D_{ala}/D_w from the MC simulation, as can be seen from table 7. The stopping power ratio obtained using the bulk density correction is more than 2% too high, furthermore the decrease with increasing energy is weaker than for the crystalline density correction. This underlines the conclusion from the previous section that for simulations of the response of the alanine dosimeter to MV x-rays, the use of the density correction for crystalline alanine is absolutely essential.

In figure 7 the relative response is displayed as a function of the CSDA range (in alanine) from table 8. Experimental photon data are represented by filled circles with error bars. Two values for electrons have been added, the experimental data are from Vörös *et al* (2012): the 6 MeV point was directly measured, the 18 MeV point is interpolated between the 16 MeV and the 20 MeV measurements from the cited paper. The experimental electron data are shown as open circles with error bars. The results of the MC simulation are represented by the filled

Table 8. Some parameters for the simulated radiation qualities: ratio of mass-energy absorption coefficients $(\mu_{en}/\rho)_{ala,W}$; stopping power ratios $s_{ala,W}$ obtained from SPRRZnrc using the two different density corrections (pellet bulk density and density of crystalline alanine); mean energy E_{av} of the secondary electrons obtained from the electron fluence spectrum using FLURZnrc and a water detector; the CSDA range in water and alanine for the given mean energies; finally the fraction f_γ of the dose due to photon interactions inside the detector volume.

Q	TPR_{10}^{20}	$(\frac{\mu_{en}}{\rho})_{ala,W}$	$s_{ala,W}$ crystal	$s_{ala,W}$ bulk	E_{av} MeV	CSDA range water in cm	CSDA range ala in cm	f_γ
^{60}Co	0.572	0.971	0.980	0.996	0.4	0.13	0.09	0.76
6 MV	0.683	0.968	0.975	0.993	1.0	0.44	0.32	0.46
8 MV	0.716	0.967	0.974	0.993	1.3	0.60	0.44	0.38
10 MV	0.733	0.966	0.973	0.993	1.5	0.71	0.52	0.34
16 MV	0.762	0.962	0.972	0.992	2.0	0.98	0.73	0.27
25 MV	0.799	0.958	0.971	0.992	2.8	1.41	1.04	0.19
6 MeV	–	–	0.969	0.991	2.7	1.35	1.00	–
18 MeV	–	–	0.969	0.990	6.6	3.35	2.49	–

triangles, the data are the same as in the previous section, with the crystalline alanine density correction. In addition, the stopping power ratio $s_{ala,W}$ relative to its value for ^{60}Co radiation is also shown.

If the CSDA range is greater than two to three times the depth of the detector which is approximately 0.5 cm, the relative response remains constant. The ratio of the stopping power ratios for both electron energies to the stopping power ratio for cobalt radiation is 0.988 (from table 8), which is identical to the average value for the relative response published by Vörös *et al* (2012).

As a conclusion, it may be stated that the energy dependence of the alanine dosimeter can be understood from the well known ratios of the mass energy absorption coefficients and the stopping power ratios for alanine and water, provided the density correction for the crystalline alanine is taken into account.

5. Summary and outlook

In order to increase the usefulness of the alanine dosimeter as a tool for quality assurance measurements in radiotherapy using MV x-rays, the response with respect to the dose to water needs to be known accurately. This quantity was determined relative to the reference quality ^{60}Co for six different qualities, namely 4, 6, 8, 10, 15 and 25 MV x-rays from clinical accelerators. The measurement series was motivated by the availability of new k_Q factors for ionization chambers with an uncertainty of 0.31% obtained from calorimetric measurements.

The measurement results seem to favour a slow decrease of the relative response from approximately 0.996 for the lower energies to 0.989 for the highest energy, 25 MV. The relative uncertainty achieved varies between 0.35% and 0.41%. The modified uncertainty budget, necessitated by new evidence as well as by a slight change in methodology is detailed in the appendix. The measured data and their uncertainties would be consistent with the assumption of an energy independent relative response of 0.993, which is in accordance with the results published by other authors. However, there are some arguments in favour of a slow decrease as observed.

Published data from NRC (Zeng *et al* 2004) have been revised using more recently available new k_Q values determined at the NRC with a lower uncertainty (McEwen 2010). The revised results agree very well with the measurement results from PTB, i.e. they also exhibit a slow decrease with increasing energy instead of remaining constant.

Monte Carlo simulations using a density correction for crystalline alanine yielded very good agreement between measured and simulated response data. This is not the case if the density correction for the bulk density of the pellet is used, as was demonstrated previously by Zeng *et al* (2005) for MeV electron radiation and confirmed by the results of Vörös *et al* (2012). This is a new result for megavoltage x-rays.

The relative response for 25 MV agrees within 0.1% with the measured and the simulated value of 0.988 for MeV electrons (Vörös *et al* 2012). This appears logical if one considers that the fraction of the dose due to secondary electrons generated within the detector volume decreases from 76% for ^{60}Co to 19% for 25 MV x-rays, i.e. the alanine dosimeter is more of a photon probe for ^{60}Co but mainly an electron probe for 25 MV, speaking in terms of Bragg–Gray theory. The fraction was also determined using Monte Carlo simulation.

In fact two different quantities are contrasted if r_Q^{MC} is compared directly to the experimental data $\langle r \rangle$: the MC simulation yields a ratio of absorbed dose values whereas the experimental data are ratios of (detected) free radical concentrations. The ratios are equal if the free radical yield, i.e. the number of free radicals generated per absorbed dose, is equal for all qualities under consideration. One could potentially combine the experimental and MC data to determine a value for the free radical yield but the overall combined uncertainty would be too large to make this a worthwhile exercise.

In summary, one may state that both the measured and the simulated data suggest that the dose-to-water response of the alanine dosimeter relative to ^{60}Co radiation decreases from $\approx$0.996 for the MV x-ray qualities with the lowest energies to a value almost equal to the relative response to MeV electrons for the highest voltages. This behaviour is well understood in terms of the stopping power ratios or the ranges of the secondary electrons, provided the density correction for the crystalline alanine is taken into account. Although, a pragmatic approach would be to use an energy-independent correction factor of 1.007 for the difference between ^{60}Co and MV photons this discards the theoretical insight that there is a slow transition from a photon detector to an electron detector. As noted earlier, for significantly different geometries of detector this transition could be very different with no 'simple' offset observed.

While bridging the gap between MV photons and MeV electrons is a very interesting result, some work remains to be done, especially concerning the response of the alanine dosimeter for the small fields employed in modern radiotherapy: the change of the radiation quality with field size may have an influence, as well as the material of the surroundings, if one aims at the verification of treatment plans in anthropomorphic phantoms. However, this will be the subject of future studies.

Acknowledgments

We wish to thank T Hackel, D-M Boche, C Makowski, K-H Mühlbradt, M Schrader and O Tappe (PTB) for their help during preparation, irradiation and measurements. We also thank J Illemann (PTB) for providing the BEAM-simulations for the *Elekta* accelerator. Thanks are due to M Krystek (PTB) for many helpful discussions as well as for having a critical eye on the uncertainty budget. Thanks are also due to P Sharpe (NPL) for providing the NPL response data as well as for helpful discussions. Inspiring discussions with V Nagy (AFRRI, USA) are also gratefully acknowledged. A part of the research presented here has received funding from

the European Commission (EC) according to the EC grant agreement no. 217257 from the Seventh Framework Programme, ERA-NET Plus.

Appendix. Uncertainty budgets and details on the experimental data

A.1. Definitions

For each specific irradiation set, a value r_j is obtained using

$$r_j = \sum_{i=1}^{n_i} w_{ji} \cdot r_{ji} \tag{A.1}$$

where r_{ji} is the response obtained from the determined dose D^{c}_{ji} for one detector and the corresponding delivered dose D_{ji} according to (3). r_j is the weighted mean (compare the appendix of Anton *et al* 2008) of the individual r_{ji}. The weights are determined by their uncertainties $u(r_{ji})$, given by

$$w_{ji} = \left(\frac{u_j}{u(r_{ji})}\right)^2 \quad \text{where} \quad u_j = \left(\sum_{i=1}^{n_i} \frac{1}{u^2(r_{ji})}\right)^{-1/2}. \tag{A.2}$$

From these data, $\langle r \rangle$ is obtained in a similar manner:

$$\langle r \rangle = \sum_{j=1}^{n_j} w_j r_j \tag{A.3}$$

where r_j is obtained from (A.1) and (A.2) and

$$w_j = \left(\frac{u}{u(r_j)}\right)^2 \quad \text{and} \quad u = \left(\sum_{j=1}^{n_j} \frac{1}{u^2(r_j)}\right)^{-1/2}. \tag{A.4}$$

If the consistency criterion (see Anton *et al* 2008, Weise and Wöger 1993)

$$q^2 < n_j - 1 \qquad \text{where} \qquad q^2 = \sum_{j=1}^{n_j} \left(\frac{r_j - \langle r \rangle}{u(r_j)}\right)^2 \tag{A.5}$$

is violated, e.g. if the uncertainties $u(r_j)$ are too small compared to the scatter of the individual values r_j, a modified value u_{mod} has to be calculated. According to Dose (2003), u_{mod} is

$$u^2_{\mathrm{mod}} = \frac{\langle r^2 \rangle - \langle r \rangle^2}{n_j - 3}, \quad \text{where} \quad \langle r^2 \rangle = \sum_{j=1}^{n_j} w_j r_j^2, \tag{A.6}$$

and w_j given by (A.4). In case (A.5) is not fulfilled, u_{mod} replaces u as the uncertainty of the weighted mean $< r >$ in the following uncertainty calculations. It has to be stressed that u_j is only a component of the combined uncertainty $u(r_j)$ and u or u_{mod} are only a component of the combined overall uncertainty of the final result.

A.2. Uncertainty budget

A.2.1. Uncertainty of the determined dose. At least three effects contribute to the uncertainty of the mass normalized amplitude A_m: the first one is the repeatability of the amplitude determination. For the chosen parameters and $D^{b} = 25$ Gy, this corresponds to 40 mGy ($= u(A_i) \cdot D^{b}$) for a single pellet or 20 mGy for an average over 4 pellets ($= u(A_m) \cdot D^{b}$). This value of $u(A_m)$ is independent of dose between 2 and 25 Gy. The second part is the variation of

Table A1. Example uncertainty budget for $D^c = \mathcal{A}_D$ for one test detector (four pellets) irradiated to a dose of 10 Gy. The left column contains a label which is referred to in the text, the middle column describes the source of the uncertainty, the right column lists the relative standard uncertainty component in per cent.

Label	Component	u_r in %
	From test detector ($n = 4$ pellets):	
1a	A_m. Amplitude repeatability	0.20
2a	A_m. Individual background	0.10
3a	A_m. Intrabatch homogeneity	0.15
4	k_T. Irradiation temperature	0.05
5	$\overline{m}$. Average mass of n probes	0.05
	Subtotal test detector	**0.28**
	From base function ($n = 4$ pellets):	
1b	A_m. Amplitude repeatability	0.08
2b	A_m. Individual background	0.04
3b	A_m. Intrabatch homogeneity	0.15
6	k_T^b. Irradiation temperature	0.05
7	$\overline{m}^b$. Average mass of n probes	0.05
	Subtotal	**0.19**
8	Systematic component	0.15
	Subtotal base function	**0.24**
9	D^b. Repeatability of irradiation	0.05
	D^b. Primary standard	0.22
	Total	**0.43**

the individual background signal which amounts to approximately 20 mGy for a single pellet (Anton 2005). The third part is the intrabatch homogeneity, i.e. the variation of the alanine content within a certain batch (see column CV in table 1). The same estimates apply to the base function amplitudes.

In table A1, an example of an uncertainty budget is given for one detector (4 pellets), irradiated to a dose of 10 Gy in the ^{60}Co reference field and is valid for the case when no calibration curve is constructed, i.e. assuming $D^c = \mathcal{A}_D$. The base functions were constructed from the spectra of one detector irradiated to 25 Gy and four unirradiated pellets as outlined above. For the higher doses, the relative uncertainty due to amplitude readout repeatability decreases, $u(A_m)$ being constant. The limiting components are the intrabatch homogeneity and an additional systematic component of 0.15%. The latter was deduced from repetitive measurements of calibration and test data sets, where the dose calculated with and without using a calibration line was compared to the known delivered dose. The non-systematic component (subtotal) for the single base of 0.19% agrees very well with type A estimates that were used in previous publications (Anton 2006). If the base is constructed from spectra of *two* irradiated detectors and eight unirradiated pellets (double base), the subtotal for the non-systematic part reduces from 0.19% to 0.14%.

Due to the time delay of less than one week between the irradiation of the calibration probes and the test probes, in all but one case fading corrections were negligible (see Anton 2006, 2008).

The uncertainty of D^c determined *with* a calibration curve is calculated only from 1a, 2a, 3a, 4 and 5 from table A1 using equation (16) from Anton (2006): all uncertainty components

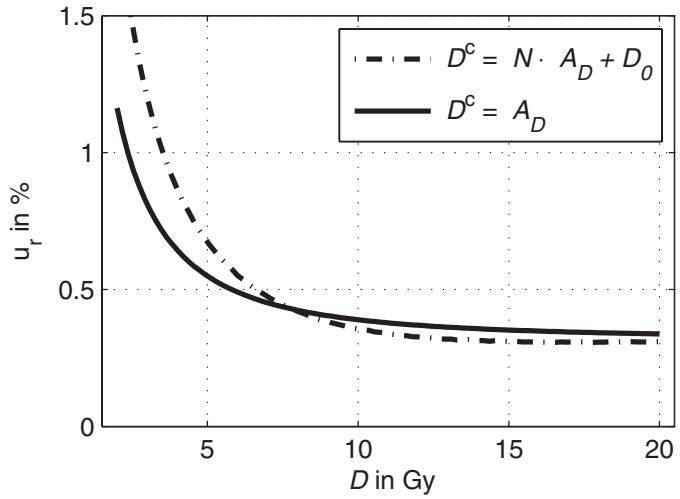

Figure A1. Relative uncertainty of the determined dose D^{c}—excluding the primary standard—with (dash-dotted curve) and without using a calibration curve (continuous curve). The data are valid for a 25 Gy base, ^{60}Co -irradiated detectors and a calibration line determined from four detectors with doses of 5, 10, 15 and 20 Gy.

associated to the base function cancel if the *same* set of base functions is used to determine the amplitude for the test- and the calibration detectors. Different from earlier work, the parameters of the calibration curve are now obtained from a linear weighted total least squares fit (Krystek and Anton 2007) to n_c data pairs $(D, \mathcal{A}_D)$ (calibration data set).

The uncertainties with and without using a calibration curve, but excluding the primary standard, are shown as a function of the delivered dose in the range between 2 Gy and 20 Gy in figure A1. The data for $D^{\mathrm{c}} = \mathcal{A}_D$ are represented by the continuous curve, the uncertainty for the determined dose using a calibration curve is displayed by the dash-dotted curve. The data are obtained using $D^{\mathrm{b}} = 25$ Gy and a calibration curve constructed from the amplitudes for four detectors irradiated with doses of 5, 10, 15 and 20 Gy. All irradiations are assumed to be carried out in the ^{60}Co reference field.

It is notable that the uncertainty for $D^{\mathrm{c}} = \mathcal{A}_D$ is lower at the low-dose end of the dose range shown. The scatter of data points at the lower end of the calibration data set may lead to larger variations of the slope and the y-axis intersection than the simple assumption of an ideal calibration curve with intersection zero and slope unity. This is still true within the range of the calibration curve ($D \geqslant 5$ Gy). However, for $D > 7$ Gy, the results obtained using a calibration curve are more accurate.

A.2.2. Uncertainty of the relative response values r_j. The variance $u^2(r_{ji}) = u^2(D^{\mathrm{c}}_{ji}) + u^2(D_{ji})$ for each individual dose is obtained as follows: for D^{c}_{ji}, components 1a, 2a, 3a, 4 and 5 from table A1 have to be taken into account. For the delivered dose D_{ji}, only the reproducibility for opening/closing the shutter (^{60}Co) and the stability of the monitor (MV x-rays) are relevant at this stage. Using these components, the weighted mean values r_j and the uncertainty component u_j are obtained.

An example is given in table A2 for $n_i = 4$ ($D_{ji} \approx 10$, 12.5, 15 and 17.5 Gy). In the upper part of the table, the left column shows the uncertainties $u(r_{ji})$ in case no calibration curve is used ($D^{\mathrm{c}} = \mathcal{A}_D$) whereas the right column shows the corresponding components in case a

Table A2. Uncertainty budget for r_j for a typical irradiation set j. Here, $n_i = 4$ test doses of approximately 10, 12.5, 15 and 17.5 Gy were chosen. The budgets for an evaluation with $D^c = \mathcal{A}_D$ (left) and using a calibration curve (right) with data points at 5, 10, 15 and 20 Gy are compared. The subtotal u_j/r_j is obtained from (A.1) and (A.2).

Component		u_r in %	
		$D^c = \mathcal{A}_D$	Calibration line
r_{j1}	($D_{j1} \approx 10$ Gy)	0.28	0.32
r_{j2}	($D_{j2} \approx 12.5$ Gy)	0.24	0.27
r_{j3}	($D_{j3} \approx 15$ Gy)	0.22	0.25
r_{j4}	($D_{j4} \approx 17.5$ Gy)	0.21	0.24
subtotal u_j/r_j		**0.12**	**0.13**
Base function		0.24	–
Reproducibility $D_{MV} = D_{ji}$			0.12
Reproducibility D_{Co}			0.05
k_T (systematic part)			0.04
$\mathbf{u(r_j)/r_j}$		**0.30**	**0.19**

calibration curve is used. In this example, a ^{60}Co calibration curve with data points at 5, 10, 15 and 20 Gy was used. The resulting relative value u_j/r_j from equations (A.1) and (A.2) is given for both cases (subtotal, printed in bold).

Where a calibration curve is not used, the uncertainty components for the base (1b, 2b, 3b, 6, 7 and 8 from table A1) have to be included after the calculation of the weighted mean r_j which yield another 0.24%.

For each irradiation set j, the positioning of the sleeve in the phantom which contains the pellets and the ionization chamber for the irradiation of the test probes was made only once, therefore this component for the uncertainty of D_{ji} has to be added *after* calculating the weighted mean r_j. A similar component associated with the reproducibility of the irradiation of calibration and base probes is also added after calculating the weighted mean because the whole set is usually irradiated without moving the sleeve. An uncertainty component for the temperature correction due to a possible systematic deviation of 0.1 K between the two different temperature sensors used at the Cobalt irradiation source and at the accelerator is included as well. Other components such as the uncertainty of the ^{60}Co calibration factor of the ionization chamber have to be added only *after* calculating the weighted mean $\langle r \rangle$ (see next section).

The example presented in table A2 is typical in the sense that the relative uncertainty of r_j is approximately 0.2% if a calibration curve is used and 0.3% for $D^c = \mathcal{A}_D$. Actual values vary slightly due to different sizes of test and calibration data sets. All results r_j and their corresponding uncertainties $u(r_j)$ are shown below in tables A3 and A4.

A.2.3. Uncertainty of the final result $\langle r \rangle$. The weighted mean values $\langle r \rangle$ were calculated from $n_j = 4$ up to $n_j = 9$ values r_j using (A.3) and (A.4). The values $u(r_j)$ listed in tables A3 and A4 served to calculate the weights according to (A.4). In addition to the uncertainty components u from equation (A.4) or u_{mod} from equation (A.6), the contributions from the ^{60}Co calibration of the ionization chamber and the k_Q-factors have to be taken into account. The uncertainty of the primary standard of 0.2% cancels because the calibration factor for the ionization chamber, the dose rate of the ^{60}Co reference field and the k_Q values were determined using the same calorimeter. The contributions to be added are finally $u_r(IC) = 0.15\%$ for the

Table A3. Relative response r_j for the irradiation sets investigated, 4 to 8 MV. Columns from left to right: nominal accelerating voltage in MV, irradiation set label, date of measurement, number of test detectors n_i (1 detector = 4 pellets); number of calibration detectors n_c; number of base detectors n_b; r_j using equations (A.1) and (A.2); the uncertainty $u(r_j)$, see section A.2.2 and the example in table A2.

MV	Set j	Date	n_i	n_c	n_b	r_j	$u(r_j)$
4	hl22	2012-03-22	4	4	1	0.9970	0.0020
4	hl22	2012-03-29	4	4	1	0.9959	0.0020
4	hl28	2012-06-26	4	5	1	0.9951	0.0020
4	hl31	2012-07-12	4	5	1	0.9931	0.0020
6	hf34	2008-06-11	5	5	1	0.9973	0.0019
6	hf37	2008-11-19	5	5	1	0.9974	0.0019
6	hj03	2009-01-30	5	5	1	0.9988	0.0019
6	hj05	2009-02-13	5	5	1	0.9988	0.0019
6	hj33	2010-10-05	6	–	2	0.9932	0.0033
6	hj37	2010-11-02	4	5	1	0.9938	0.0021
6	hj38	2010-11-18	4	–	2	0.9942	0.0030
6	hj45	2011-03-23	4	4	2	0.9967	0.0030
6	hj45	2011-03-31	4	5	1	0.9978	0.0021
8	hj31	2010-09-15	6	–	1	0.9908	0.0033
8	hj39	2010-12-14	8	–	1	0.9910	0.0033
8	hj49	2011-05-18	5	6	1	0.9954	0.0019
8	hl01	2011-06-22	5	6	1	0.9952	0.0018
8	hl22	2012-03-29	4	4	1	1.0004	0.0020

Table A4. Relative response r_j for the irradiation sets investigated, 10 to 25 MV. Columns from left to right: nominal accelerating voltage in MV, irradiation set label, date of measurement, number of test detectors n_i (1 detector = 4 pellets); number of calibration detectors n_c; number of base detectors n_b; r_j using equations (A.1) and (A.2); the uncertainty $u(r_j)$, see section A.2.2 and the example in table A2.

MV	Set j	Date	n_i	n_c	n_b	r_j	$u(r_j)$
10	hf34	2008-05-29	4	4	1	0.9943	0.0021
10	hf36	2008-07-22	5	5	1	0.9954	0.0052
10	hf37	2008-11-13	5	5	1	0.9939	0.0019
10	hj03	2008-12-16	5	5	1	0.9929	0.0019
10	hj07	2009-03-12	6	5	1	0.9937	0.0019
10	hj41	2011-01-06	4	5	1	0.9897	0.0021
10	hj45	2011-03-23	4	–	2	0.9958	0.0030
10	hj45	2011-03-30	4	6	1	0.9987	0.0021
15	hl15	2012-01-24	6	–	2	0.9915	0.0027
15	hl15	2012-01-26	3	–	2	0.9900	0.0028
15	hl15	2012-01-26	3	–	2	0.9899	0.0029
15	hl16	2012-02-09	6	–	1	0.9880	0.0029
15	hl16	2012-02-14	6	–	1	0.9901	0.0030
15	hl20	2012-03-02	3	4	1	0.9864	0.0021
25	hj29	2010-08-18	6	–	2	0.9860	0.0029
25	hj32	2010-09-29	8	–	1	0.9921	0.0033
25	hj34	2010-10-13	8	–	1	0.9935	0.0033
25	hj49	2011-05-17	5	6	1	0.9918	0.0019
25	hl01	2011-06-17	5	6	1	0.9867	0.0018
25	hl03	2011-08-09	4	6	1	0.9883	0.0019
25	hl09	2011-11-02	3	–	2	0.9906	0.0028

calibration factors and $u_r(k_Q) = 0.31\%$ for the quality correction factors of the ionization chamber(s).

A.3. Details of the experimental results

The results of each individual irradiation and measurement set j are listed in tables A3 and A4. The first column lists the nominal accelerating voltage in MV, the second one a label attached to each irradiation set[8] and the third column contains the date of measurement. The following three columns describe the size of the dataset: n_i is the number of test detectors irradiated in the MV x-ray field. Their doses are always interspersed between the lowest and the highest dose of the calibration set. The latter consisted of n_c probes with doses between 5 and 25 Gy. n_b is the number of base detectors. $n_\mathrm{b} = 2$ means that there were spectra from two irradiated detectors and eight unirradiated pellets used to construct the base functions. The individual relative response values r_j are listed in the following column and were obtained using equations (A.1) and (A.2). The uncertainties of these values are denoted as $u(r_j)$ and are listed in the rightmost column. The calculation of these values is described in section A.2.2, an example is given in table A2.

With a calibration curve, the uncertainty of the individual values is approximately 0.2% whereas the quicker evaluation without a calibration curve leads to a higher uncertainty of approximately 0.3%. For the latter case, it appears to be insignificant whether a single ($n_\mathrm{b} = 1$) or a double ($n_\mathrm{b} = 2$) set of pellets was used for the construction of the base functions. There appears to be no correlation between the value of r_j and whether or not a calibration curve was employed. The uncertainties are in general slightly smaller if the data sets are bigger, which is no surprise. However, a small set of test data ($n_i = 3$) evaluated *with* a calibration curve yields more accurate results than a large set ($n_i = 8$) evaluated without. The higher value of $u(r_j)$ for the 10 MV set hf36 is due to a fading correction and its associated uncertainty.

References

Aalbers A H L, Hoornaert M-T, Minken A, Palmans H, Pieksma M W H, de Prez L A, Reynaert N, Vynckier S and Wittkämper F W 2008 Code of practice for the absorbed dose determination in high energy photon and electron beams *NCS Report*18 *Nederlandse Commissie voor Stralingsbescherming*

Anton M 2005 Development of a secondary standard for the absorbed dose to water based on the alanine EPR dosimetry system *Appl. Radiat. Isot.* **62** 779–95

Anton M 2006 Uncertainties in alanine/ESR dosimetry at PTB *Phys. Med. Biol.* **51** 5419–40

Anton M 2008 Postirradiation effects in alanine dosimeter probes of two different suppliers *Phys. Med. Biol.* **53** 1241–58

Anton M, Kapsch R P, Krystek M and Renner F 2008 Response of the alanine/ESR dosimetry system to MV x-rays relative to ^{60}Co radiation *Phys. Med. Biol.* **53** 2753–70

Berger M, Coursey J S, Zucker M A and Chang J 2005 ESTAR, PSTAR, and ASTAR: computer programs for calculating stopping-power and range tables for electrons, protons, and Helium ions (version 1.2.3) *Technical Report* (Gaithersburg, MD: National Institute of Standards and Technology) http://www.nist.gov/pml/data/star/index.cfm

Bergstrand E S, Shortt K R, Ross C K and Hole E O 2003 An investigation of the photon energy dependence of the EPR alanine dosimetry system *Phys. Med. Biol.* **48** 1753–71

Budgell G, Berresford J, Trainer M, Bradshaw E, Sharpe P and Williams P 2011 A national dosimetric audit of IMRT *Radiother. Oncol.* **99** 246–52

De Angelis C, De Coste V, Fattibene P, Onori S and Petetti E 2005 Use of alanine for dosimetry intercomparisons among italian radiotherapy centers *Appl. Radiat. Isot.* **62** 261–5

Ding G X, Rogers D W O and Mackie T R 1995 Calculation of stopping-power ratios using realistic clinical electron beams *Med. Phys.* **22** 489–501

[8] hf: from batch AF594, hj: from batch AJ598, hl: from batch AL595.

Dose V 2003 Bayesian inference in physics: case studies *Rep. Prog. Phys.* **66** 1421–61

Garcia T, Lacornerie T, Popoff R, Lourenço V and Bordy J-M 2011 Dose verification and calibration of the cyberknife® by EPR/alanine dosimetry *Radiat. Meas.* **46** 952–7

Hubbell J H 1982 Photon mass attenuation and energy-absorption coefficients from 1 keV to 20 MeV *Appl. Radiat. Isot.* **33** 1269–90

ICRU 1984 Stopping powers for electrons and positrons *ICRU Report No. 37* (Washington, DC: ICRU)

JCGM100 2008 Evaluation of measurement data—guide to the expression of uncertainty in measurement. GUM 1995 with minor corrections *Technical Report* JCGM 100, Working Group 1 of the Joint Committee for Guides in Metrology JCGM/WG 1

Kawrakow I 2000 Accurate condensed history Monte Carlo simulation of electron transport: I. EGSnrc, the new EGS4 version *Med. Phys.* **27** 485–98

Kawrakow I, Mainegra-Hing E, Rogers D W O, Tessier F and B Walters B R 2010 The EGSnrc code system: Monte Carlo simulation of electron and photon transport *NRC Report* PIRS-701 (Ottawa, Canada: NRCC)

Krauss A 2006 The PTB water calorimeter for the absolute determination of absorbed dose to water in ^{60}Co radiation *Metrologia* **43** 259–72

Krauss A and Kapsch R-P 2007 Calorimetric determination of k_Q factors for NE 2561 and NE2571 ionization chambers in 5 cm × 5 cm and 10 cm × 10 cm radiotherapy beams of 8 MV and 16 MV photons *Phys. Med. Biol.* **52** 6243–59

Krystek M and Anton M 2007 A weighted total least-squares algorithm for fitting a straight line *Meas. Sci. Technol.* **18** 1–5

Krystek M and Anton M 2011 A least-squares algorithm for fitting data points with mutually correlated coordinates to a straight line *Meas. Sci. Technol.* **22** 1–9

McEwen M R 2010 Measurement of ionization chamber absorbed dose k_Q factors in megavoltage photon beams *Med. Phys.* **37** 2179–93

McEwen M, Sephton J and Sharpe P 2006 Alanine dosimetry for clinical applications *Technical Report PTB-Dos-51, Physikalisch-Technische Bundesanstalt* pp 9–14

Muir B, McEwen M R and Rogers D W O 2011 Monte Carlo calculations of the beam quality conversion factor k_Q for cylindrical ionization chambers: comparison with published data *Med. Phys.* **38** 4600–9

Onori S, Bortolin E, Calicchia A, Carosi A, De Angelis C and Grande S 2006 Use of commercial alanine and TL dosemeters for dosimetry intercomparisons among italian radiotherapy centres *Radiat. Prot. Dosim.* **120** 226–9

Picard S, Burns D T, Roger P, Allisy-Roberts P J, Kapsch R-P and Krauss A 2011 Key comparison BIPM.RI(I)-K6 of the standards for absorbed dose to water of the PTB, Germany and BIPM in accelerator photon beams *Metrologia* **48** 06020

Picard S, Burns D T, Roger P, Allisy-Roberts P J, McEwen M R, Cojocaru C D and Ross C K 2010 Comparison of the standards for absorbed dose to water of the NRC and the BIPM for accelerator photon beams *Metrologia* **47** 06025

Rogers D W O, Walters B and Kawrakow I 2004 BEAMnrc User's Manual *NRC Report* PIRS 509(a)revH (Ottawa, Canada: NRCC)

Schaeken B, Cuypers R, Lelie S, Schroeyers W, Schreurs S, Janssens H and Verellen D 2011 Implementation of alanine/EPR as transfer dosimetry system in a radiotherapy audit programme in Belgium *Radiother. Oncol.* **99** 94–96

Seltzer S M 1993 Calculation of photon mass energy-transfer and mass energy-absorption coefficients *Radiat. Res.* **136** 147–70

Sharpe P H G 2003 Progress report on radiation dosimetry at NPL *Technical Report* (Sèvres: BIPM)

Sharpe P H G 2006 Alanine dosimetry for clinical applications *Technical Report* PTB-Dos-51, Physikalisch-Technische Bundesanstalt pp 3–8

Sharpe P H G, Rajendran K and Sephton J P 1996 Progress towards an alanine/ESR therapy level reference dosimetry service at NPL *Appl. Radiat. Isot.* **47** 1171–5

Sheikh-Bagheri D and Rogers D W O 2002 Monte Carlo calculations of nine megavoltage photon beam spectra using the BEAM code *Med. Phys.* **29** 391–402

Vörös S, Anton M and Boillat B 2012 Relative response of alanine dosemeters for high-energy electrons determined using a Fricke primary standard *Phys. Med. Biol.* **57** 1413–32

Weise K and Wöger W 1993 A Bayesian theory of measurement uncertainty *Meas. Sci. Technol.* **4** 1–11

Zeng G G, McEwen M R, Rogers D W O and Klassen N V 2004 An experimental and Monte Carlo investigation of the energy dependence of alanine/EPR dosimetry: I. Clinical x-ray beams *Phys. Med. Biol.* **49** 257–70

Zeng G G, McEwen M R, Rogers D W O and Klassen N V 2005 An experimental and Monte Carlo investigation of the energy dependence of alanine/EPR dosimetry: II. Clinical electron beams *Phys. Med. Biol.* **50** 1119–29